



ELSEVIER

Available online at www.sciencedirect.com

SCIENCE @ DIRECT®

Ocean Engineering 32 (2005) 1608–1622

OCEAN
ENGINEERING

www.elsevier.com/locate/oceaneng

Probabilistic determination of critical wave height for a multi-degree of freedom capsizing model

Leigh McCue^{*,a}, Armin Troesch^b

^a*Aerospace and Ocean Engineering, Virginia Tech, Blacksburg, VA 24061–0203, USA*

^b*Department of Naval Architecture and Marine Engineering, University of Michigan, 2600 Draper Road, Ann Arbor, MI 48109, USA*

Received 1 June 2004; accepted 6 October 2004

Available online 2 March 2005

Abstract

In this paper a statistical methodology is extended to the nonlinear multi-degree of freedom vessel capsizing problem in random seas. It is demonstrated that the study of transient motions, through analysis of the erosion of the vessel's safe basin mapped in the space of initial conditions [Soliman, M.S. Thompson, J., 1991. Transient and steady state analysis of capsizing phenomena. *Applied Ocean Research* 13, 2], leads to significantly less conservative and potentially more accurate predictions of ultimate dynamic stability. The work presented herein pairs this approach with a statistical framework to yield feasible stability criteria.

© 2005 Elsevier Ltd. All rights reserved.

Keywords: Capsizing; Multiple degrees of freedom; Safe basin; Integrity curve; Probability density function; Random seas

1. Introduction

The problem of vessel capsizing has plagued mariners for centuries. While modern United States Coast Guard stability criteria are principally a static measure, it has been demonstrated that large amplitude roll motions and capsizing are very much a dynamic phenomena with strong nonlinearities and chaotic behavior, e.g. Soliman and Thompson (1991) or Falzarano et al. (1992). Engineers and applied mathematicians have experimented

* Corresponding author. Tel.: +1 540 231 4351.

E-mail address: mccue@vt.edu (L. McCue).

with a large range of numerical, experimental, and analytical methods to improve predictive capabilities for capsizes.

Haddara and colleagues at Memorial University of Newfoundland have progressed in using parametric models for estimating crucial vessel parameters including employing neural networks techniques. They have applied this approach to time-domain simulations of transverse stability to demonstrate in a limited sense viable comparison to experimental results of full scale vessel performance in random seas (Zhang and Haddara, 1993; Haddara et al., 1994; Haddara and Wishahy, 2002). However, this approach has not been demonstrated for large amplitude motions leading to capsizes and may be time-consuming and ineffective to employ in a regulatory form.

Another methodology, first used for the capsizes problem by Thompson et al. (1987) and Falzarano et al. (1992) involves the use of Melnikov methods to predict chaotic bifurcations in space for both a heteroclinic model emulating symmetric vessel capsizes and a homoclinic model representing a vessel with an initial bias due to factors such as water on deck, damage, or wind heel angle. While closed form solutions such as those presented by the use of Melnikov's method are the most feasible for developing an improved and safer regulatory basis, the method has restrictive limitations. Because Melnikov's method treats forcing and damping as perturbations from a mean, it is difficult, if not impossible to apply it to a multi-degree of freedom model with large forcing without detailed mathematical manipulation and reduction of variables (Chen et al., 1999), again making this approach impractical in a regulatory sense.

However, with a comparative basis in his work with Melnikov methods, Thompson and collaborators developed and established the use of safe basins and integrity curves in analyzing capsizes for one degree of freedom models (Soliman and Thompson, 1991; Spyrou and Thompson, 2000; Thompson, 1997). These methods employing safe basins are essentially numerical studies and as such are not constrained to small damping and forcing as required by the closed-form Melnikov methods. The concept behind the integrity curve approach is one of plotting the phase space of roll motion initial conditions and then finding the ratio of safe area to capsizes area for a given wave height thus yielding an 'integrity' value. A range of wave heights may be considered allowing one to produce a series of 'integrity' values in the form of an 'integrity' curve. Under traditional examination of these curves one typically finds a 'critical' wave height for which there is a rapid loss of stability (Thompson, 1997).

This process of constructing an integrity curve is completed by sampling the state space for safe/capsizes results at a given time, or phase relative to the forcing wave. For a simple periodic system, this shift in phase can be considered as either a change in phase of the forcing, or a shift in the initial condition of the sampled parameter, e.g. initial release angle for the case of a forced pendulum. Examine, for example, Fig. 1. Σ_0 and Σ_1 represent two cross-sections of a periodic trajectory taken at different points in the trajectory. For this simple diffeomorphic process, discussed in Wiggins (1990) and given by Eq. (1) below, the two open sets V_0 and V_1 in Σ_0 and Σ_1 , respectively, can either be interpreted as an offset in initial conditions or as a shift in sampling phase. In the notation of Wiggins, if one defines P_0 and P_1 as the Poincaré maps of the open sets denoted by V_0 and V_1 , and $\phi(t,x)$ as the flow generated by Eq. (1), one can represent the mappings by Eq. (2)

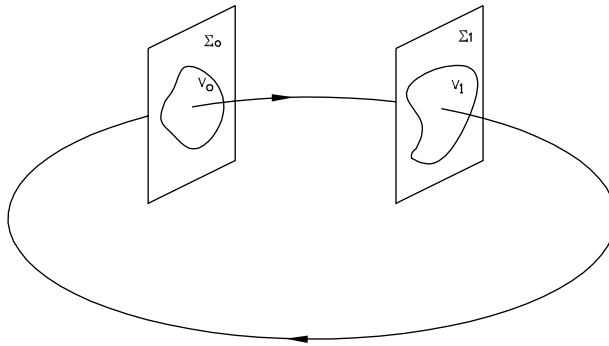


Fig. 1. Two sample cross-sections for an arbitrary periodic trajectory (Wiggins, 1990).

(Wiggins, 1990)

$$\dot{x} = f(x), \quad x \in \mathbb{R}^n, \quad \text{where } f : U \rightarrow \mathbb{R}^n \text{ is } C^r \text{ on } U \subset \mathbb{R}^n \quad (1)$$

$$P_0 : V_0 \rightarrow \Sigma_0; \quad x_0 \mapsto \phi(\tau(\bar{x}_0), \bar{x}_0), \quad \bar{x}_0 \in V_0 \subset \Sigma_0, \quad (2)$$

$$P_1 : V_1 \rightarrow \Sigma_1; \quad x_1 \mapsto \phi(\tau(\bar{x}_1), \bar{x}_1), \quad \bar{x}_1 \in V_1 \subset \Sigma_1$$

By viewing the mapping in this mathematical context, the importance of phase, for this simple example, becomes clear. Due to the explicit time dependence on the spatial coordinate in Eq. (2), i.e. $\tau(\bar{x})$ or the time of first return of x to Σ , the equivalence between a shift of phase versus initial condition is apparent. Physically in the example of vessel capsizing in beam seas, this phase/initial condition shift corresponds to considering the vessel's position relative to the forcing wave surface which can be represented either as a shift in time of excitation or a change in the lateral degree of freedom along the wave surface, namely sway.

In works by Lee et al. (accepted for publication), McCue and Troesch (2003) and Obar et al. (2001) the integrity curve concept was extended to a three degree of freedom, six state variables model. When integrity curves for an entire six state variable space are considered, one finds a significant range of 'critical' wave heights based upon chosen initial conditions. The mapping associated with the multi-degree of freedom system in Eq. (3), Section 2, is no longer a diffeomorphism as neither it nor its inverse are differentiable, or of class C^r (Marsden and Ratiu, 1991). Physically this corresponds to the fact that while mapped points not leading to capsizing stay within a small region near equilibrium, points leading to capsizing leave the open set near equilibrium towards an unsafe basin of attraction. However, while the process is not diffeomorphic, an analogous relation between sway initial condition and phase of the forcing waves as discussed above is applicable. In fact, this proves to be a crucial aspect of the model with ultimate stability being highly dependent upon sway initial condition/phase. As an example, if sway initial condition is taken to be zero, corresponding to zero phase relative to the wave crest, the vessel could be safe for large wave amplitudes and yet for a sway offset of half a wave length the same vessel in the same sea state may capsize for any roll initial condition pair (Lee et al., accepted for publication; McCue and Troesch, 2003).

For real ships in a real seaway this point may be viewed as academic, at best. A safe vessel in a particular sea state will need be stable for any excitation phase relative to a wave crest and thus for any initial sway. One wishes, for operational guidance and simplicity, to determine a maximal value for critical wave height in any expected sea state. From the safety perspective it is natural to choose the lowest value encountered at which there is a rapid loss of stability. However, from the operator perspective such a minimal value may be unreasonably low. The question is then posed as to how to predict minimum safe wave heights while avoiding being excessively and impractically cautious. Additionally, the traditional safe basin integrity curve value is based upon a relatively arbitrary range of roll and roll velocity initial conditions. It is the purpose of this work to eliminate such an arbitrary basis and follow instead a statistical model, similar to that employed by (Schauer et al., 1995), to indicate prudent critical wave height regimes.

Probabilistic methods have been employed in combination with Melnikov function approaches (Hsieh et al., 1994; Schauer et al., 1995). Additionally, probabilistic approaches have been used to analyze the impact of uncertainties in design variables relevant to stability (Atua and Ayyub, 1997). In Belenky (2000) a probabilistic approach is used to assess past and present work which could lead to a refined stability standard accounting for various factors (e.g. loading and human error) as well as mechanisms of capsizing such as quartering seas, green water on deck, and broaching. However, no one has presented a computationally feasible, experimentally validated, and statistically reliable methodology that could be used to improve upon or redefine existing capsizing regulations with regard to initial condition space. At the *Eighth International Conference on the Stability of Ships and Ocean Vehicles*, McCue and Troesch presented a form of multi-degree of freedom integrity curves and discussed potential use of this concept coupled with statistical analysis to predict maximal operational wave heights for anticipated roll motions and initial condition parameters (McCue and Troesch, 2003). This work serves as an extension of that premise analyzing barge motions within one, two, or three standard deviations from the average value for a given sea state. The data presented is for a simple geometry of realistic dimensions for a vessel operated in conditions found on an annual basis in the North Atlantic.

2. Model

The quasi-nonlinear three degree of freedom model developed and validated by Lee and others (Lee et al., accepted for publication; McCue and Troesch, 2003; Obar et al., 2001) was used to analyze a low freeboard box barge model with principal dimensions defined in Fig. 2, angle of vanishing stability of 31.7° , and V_{cg} at the mean water line. The quasi nonlinear model is a three degree of freedom 'blended' hydrodynamic model designed to simulate highly nonlinear roll motion of a box barge. The model employs the use of an effective gravitational field to account for the centrifugal forces due to the circular water particle motion in addition to the earth's gravitational field. Details of this process can be found in Lee et al. (accepted for publication) and McCue and Troesch (2003). Implicit in the model is a long wave assumption. The numerical model also accounts

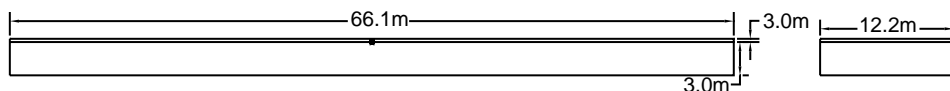


Fig. 2. Principal dimensions of box barge model.

for the hydrostatic effects of water on deck due to deck immersion but does not account for the dynamics of water on deck. A great deal of literature exists treating the dynamics of water on deck. Most notably, Dillingham used Glimm's method to analyze dynamic effects of water on deck for a linear two degree of freedom model with coupling in sway and roll under the assumption of shallow water theory (Dillingham, 1981). This work was extended to a six degree of freedom linearized ship model by Laranjinha et al. (2002). These works produce results for nonlinear motions but do not present data for vessel capsizing. While the method of Laranjinha et al. (2002) has proven to attain interesting results for investigating the higher order effects of water on deck, it is generally too computationally intensive to incorporate into a nonlinear ship capsizing model where the deck edges are frequently immersed. Other multiple degree of freedom models that are able to simulate dynamics of water on deck run considerably slower than real time and have only limited experimental validation (Belenky et al., 2002). Solving the two coupled problems of nonlinear ship motions with dynamics of water on deck is prohibitively time-intensive for generating the volume of data needed to complete the work presented here. The experimentally validated, 'blended' model of Eq. (3) simulates hours of data in seconds allowing one to generate years of real time data in a matter of days (Lee et al., accepted for publication; McCue and Troesch, 2003). Thus the principal use of the numerical simulator described herein is to focus upon the nonlinear motions of the vessel including the first order hydrostatic influence of water on deck leading to capsize.

The equations of motion in the inertial coordinate system employed by this quasi-nonlinear model are given in Eq. (3) where subscripts 2, 3, and 4 represent sway, heave and roll degrees of freedom, respectively. For each sea state considered, the linear ship motions program SHIPMO (Beck and Troesch, 1990) was used to generate added mass, damping, and diffraction force coefficients in addition to response amplitude operators for linear vessel motions as is discussed in greater detail in Sections 3 and 4

$$\begin{aligned}
 & \begin{bmatrix} m + a_{22} & 0 & a_{24} \\ 0 & m + a_{33} & 0 \\ a_{42} & 0 & I_{cg} + a_{44} \end{bmatrix} \begin{pmatrix} \ddot{x}_g \\ \ddot{y}_g \\ \ddot{\theta} \end{pmatrix} + \begin{bmatrix} b_{22} & 0 & b_{24} \\ 0 & b_{33} & 0 \\ b_{42} & 0 & b_1 \end{bmatrix} \begin{pmatrix} \dot{x}_g \\ \dot{y}_g \\ \dot{\theta} \end{pmatrix} \\
 & + \begin{bmatrix} 0 & 0 & 0 \\ 0 & 0 & 0 \\ 0 & 0 & b_2 \end{bmatrix} \begin{pmatrix} 0 \\ 0 \\ \dot{\theta}|\dot{\theta}| \end{pmatrix} = \begin{pmatrix} \rho g_{e2} \nabla + f_2^D \\ \rho g_{e3} \nabla - mg + f_3^D \\ \rho g_{e4} GZ \nabla + f_4^D \end{pmatrix} \quad (3)
 \end{aligned}$$

An explanation of terms is as follows with a table of values presented in Tables 1 and 2:

Table 1

Mass coefficient values used in equations of motion for each sea excitation frequency

Mean wave period (s)	m (kg/m)	a_{22}/m	$a_{24}/(mB)$	$a_{33}/(m)$	$a_{42}/(mB)$	$a_{44}/(mB^2)$	$I_{cg}/(mB^2)$
3.2	37,155	0.0527	0.0157	1.7983	0.0157	0.0581	0.1225
4.8	37,155	0.3272	0.0233	1.4998	0.0233	0.0567	0.1225
6.3	37,155	0.7041	-0.0025	1.4932	-0.0025	0.0578	0.1225
7.5	37,155	0.8640	-0.0215	1.6009	-0.0215	0.0596	0.1225
8.8	37,155	0.8932	-0.0301	1.7686	-0.0301	0.0607	0.1225
9.7	37,155	0.8766	-0.0314	1.8976	-0.0314	0.0608	0.1225
10.9	37,155	0.8516	-0.0317	2.0790	-0.0317	0.0612	0.1225
12.4	37,155	0.8123	-0.0300	2.3282	-0.0300	0.0612	0.1225
13.8	37,155	0.7873	-0.0284	2.5107	-0.0284	0.0611	0.1225
15.0	37,155	0.7671	-0.0272	2.6713	-0.0272	0.0607	0.1225
16.4	37,155	0.7469	-0.0259	2.8521	-0.0259	0.0601	0.1225
18.0	37,155	0.7326	-0.0248	3.0566	-0.0248	0.0601	0.1225
20.0	37,155	0.7231	-0.0238	3.3367	-0.0238	0.0606	0.1225

 x sway degree of freedom y heave degree of freedom θ roll degree of freedom a_{ij}, b_{ij} added mass and damping coefficients f_j^D diffraction forces b_1 and b_2 linear and nonlinear roll damping coefficients g_{e_i} time dependent sway and heave components of effective gravity ∇ time dependent volume of hull including possibility for deck immersion and bottom emersion

GZ time dependent roll righting arm

Table 2

Damping coefficient values used in equations of motion for each sea excitation frequency

Mean wave period (s)	$b_{22}/(mw)$	$b_{24}/(mwB)$	$b_{33}/(mw)$	$b_{42}/(mwB)$	$b_1/(mwB^2)$	$b_2/(mB^2)$
3.2	0.3498	0.0055	0.0784	0.0055	0.0001	0.1871
4.8	0.6492	-0.0256	0.5311	-0.0256	0.0012	0.1871
6.3	0.6130	-0.0432	1.0542	-0.0432	0.0034	0.1871
7.5	0.4402	-0.0380	1.4146	-0.0380	0.0037	0.1871
8.8	0.2733	-0.0266	1.7366	-0.0266	0.0029	0.1871
9.7	0.1995	-0.0204	1.9186	-0.0204	0.0024	0.1871
10.9	0.1246	-0.0136	2.1460	-0.0136	0.0017	0.1871
12.4	0.0703	-0.0081	2.3965	-0.0081	0.0011	0.1871
13.8	0.0491	-0.0058	2.5486	-0.0058	0.0009	0.1871
15.0	0.0368	-0.0044	2.6562	-0.0044	0.0071	0.1871
16.4	0.0286	-0.0035	2.7591	-0.0035	0.0006	0.1871
18.0	0.0208	-0.0025	2.8850	-0.0025	0.0005	0.1871
20.0	0.1111	-0.0014	3.0661	-0.0014	0.0003	0.1871

3. Sea state statistics

The linear ship motions program SHIPMO (Beck and Troesch, 1990) was used to generate the ISSC spectral density functions (SDF) for the wave conditions defined by the parameters in Table 3. This collection of sea states was chosen from historical data in the North Atlantic Ocean to be representative of realistic environments (Bales et al., 1981). Assuming the process is narrow banded and normally distributed allows one to generate the Rayleigh probability density function (PDF) of the envelope curve. The root mean square for a narrow banded, normally distributed, sea state with given significant wave height is given by $\sigma = h_{1/3}/4$, where σ and $h_{1/3}$ represent standard deviation and significant wave height, respectively. The return period associated with a height can be determined by the equation $\tilde{\zeta}_{1/k} = \sigma\sqrt{2 \ln k}$ with k denoting the number of cycles to reach a certain wave amplitude. This translates directly to time by multiplying the number of cycles by the mean period of the process. Therefore one can find the probability of meeting or exceeding any given wave height as being $1/k$ which is expressed in Eq. (4):

$$P(\tilde{\zeta} \geq \tilde{\zeta}_{1/k}) = \exp\left(-\frac{(\tilde{\zeta}_{1/k}/\sigma)^2}{2}\right) \quad (4)$$

According to Soliman and Thompson's work for a single degree of freedom model, it is shown that if a vessel shall capsize, it is likely to capsize within four wave cycles and has indistinguishable capsize behavior between analysis of 8–16 wave cycles (Soliman and Thompson, 1991). The results presented in this study were indeed consistent with this statement with the majority of capsize events occurring within one to two cycles and nearly all occurring within eight wave cycles. For this statistical analysis the probability of meeting or exceeding a critical wave height in the given sea state n consecutive times is considered. In this notation n denotes the number of wave cycles with height equal to or greater than $2\tilde{\zeta}_{1/k}$ leading to capsize. Each wave encounter is treated as an independent, random event described by a Rayleigh PDF. As an example, curves representing

Table 3
Sea state data used in analysis

Mean wave period (s)	Significant wave heights (m)
3.2	0.91, 1.52
4.8	0.91, 1.83, 2.74
6.3	0.91, 1.83, 2.74
7.5	0.91, 1.83, 2.74, 3.66
8.8	0.91, 1.83, 2.74, 3.66, 4.57
9.7	0.91, 1.83, 2.74, 3.66, 4.57, 5.49
10.9	0.91, 1.83, 2.74, 3.66, 4.57, 5.49, 6.40
12.4	0.91, 1.83, 2.74, 3.66, 4.57, 5.49, 6.40, 7.32
13.8	0.91, 1.83, 2.74, 3.66, 4.57, 5.49, 6.40, 7.32, 8.23
15.0	0.91, 1.83, 2.74, 3.66, 4.57, 5.49, 6.40, 7.32, 8.23, 9.14
16.4	0.91, 1.83, 2.74, 3.66, 4.57, 5.49, 6.40, 7.32, 8.23, 9.14, 10.06, 10.97, 11.89
18.0	0.91, 1.83, 2.74, 3.66, 4.57, 5.49, 6.40, 7.32, 8.23, 9.14, 10.06, 10.97, 11.89, 12.80, 13.72, 14.02
20.0	0.91, 1.83, 2.74, 3.66, 4.57, 5.49

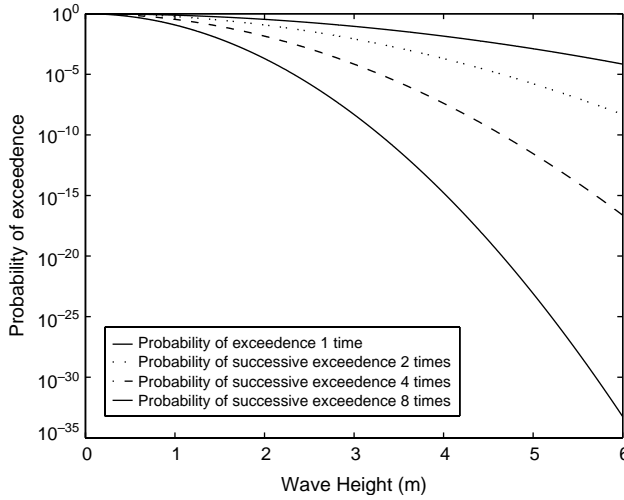


Fig. 3. Probability of exceeding given wave amplitude 1, 2, 4, and 8 times in succession for a significant wave height of 2.74 m and mean period of 15 s.

the probability of a group of waves defined as one, two, four or eight waves in succession exceeding a given wave height in a sea state described by a significant wave height and mean wave period of 2.74 m and 15 s are shown in Fig. 3. This wave height and frequency pair represents a typical statistically likely sea state encountered on an annual basis in the North Atlantic Ocean (Bales et al., 1981).

4. Roll angle statistics

Based upon the output spectral density function for roll motion generated by SHIPMO (Beck and Troesch, 1990) one can generate probability density functions for both roll and roll velocity motion from Eqs. (5)–(8)

$$\sigma_{\theta}^2 = \int_0^{\infty} S_{\theta}^+(\omega) d\omega \tag{5}$$

$$\sigma_{\dot{\theta}}^2 = \int_0^{\infty} \omega^2 S_{\theta}^+(\omega) d\omega \tag{6}$$

$$P_{\theta}(\theta) = \frac{1}{\sigma_{\theta}\sqrt{2\pi}} \exp\left(-\frac{1}{2}\right) \left(\frac{\theta}{\sigma_{\theta}}\right)^2 \tag{7}$$

$$P_{\dot{\theta}}(\dot{\theta}) = \frac{1}{\sigma_{\dot{\theta}}\sqrt{2\pi}} \exp\left(-\frac{1}{2}\right) \left(\frac{\dot{\theta}}{\sigma_{\dot{\theta}}}\right)^2 \tag{8}$$

Since it is assumed in this paper that the roll response is a stationary random process with mean value zero, it is known that θ and $\dot{\theta}$ are uncorrelated and the joint PDF is given by Eq. (9) (Crandall and Mark, 1963; Newland, 1993)

$$P_{\theta\dot{\theta}}(\theta, \dot{\theta}) = P_{\theta}(\theta)P_{\dot{\theta}}(\dot{\theta}) \quad (9)$$

As an example, Fig. 4 presents the joint PDF for roll and roll velocity for the sea state given by a significant wave height of 2.74 m with a mean period of 15 s.

Francescutto's work notes that it is not at all unlikely for a Gaussian input to return a distinctly non-Gaussian output (Francescutto, 1993). In particular, he presents a single degree of freedom roll model subject to narrow banded excitation which yields non-Gaussian roll responses with 'soft' memory of initial conditions (Francescutto, 1993). Clearly the work presented herein is a simplification. The loss of stability is so abrupt due to low freeboard and static water on deck that numerical investigations did not exhibit the traditional softening spring behavior found in Francescutto (1993). It is our hypothesis that the backbone response is detectable in only a relatively small parameter region for the analyzed vessel geometry. Forcing of sufficiently large amplitude to produce the traditional backbone type response in other ship hull forms led to capsize for the studied barge. The model behaved nearly linearly up to the angle of deck immersion and capsized soon thereafter thus providing the justification for the assumptions that led to Eqs. (7)–(9).

5. Probability of capsizing

Using the quasi-nonlinear three degree of freedom simulation model described in detail in Lee et al. (accepted for publication), a safe basin phase space portrait is generated setting all initial conditions except roll and roll velocity to zero (e.g. $x(0)$, $\dot{x}(0)$, $y(0)$, $\dot{y}(0) = 0$). By varying the incident wave heights, this process allows one to create the traditional integrity curve of the works of Thompson et al. (Soliman and Thompson, 1991; Thompson, 1997). For the work presented here a modification to this approach is undertaken.

Again one begins with the safe basin, however, in this case the standard deviation of roll and roll velocity initial conditions is noted. For example, Fig. 5 presents the safe basin phase space for the model in twelve regular wave conditions of constant frequency and heights up to and above the significant wave height of 2.74 m. The three concentric ellipses denote one, two, and three standard deviations in roll and roll velocity initial conditions as determined from the SHIPMO output for a seastate defined by $h_{1/3} = 2.74$ m and $t_e = 15$ s. For the PDF used here, 68% of all initial conditions fall within one standard deviation of the mean. Similarly, 95 and 99% of all initial conditions for roll and roll velocity will fall within two and three standard deviations, respectively, of the mean notated by the outer two concentric ellipses. The probability of attaining these sea states below the significant wave height as well as the probability of capsizing at these given wave heights are cumulated.

Based upon this knowledge, weighted integrity curves can be generated by following such a process for multiple wave heights. As discussed in Section 3, it is a relatively straight-forward matter to calculate the probability of encountering n waves of equal or

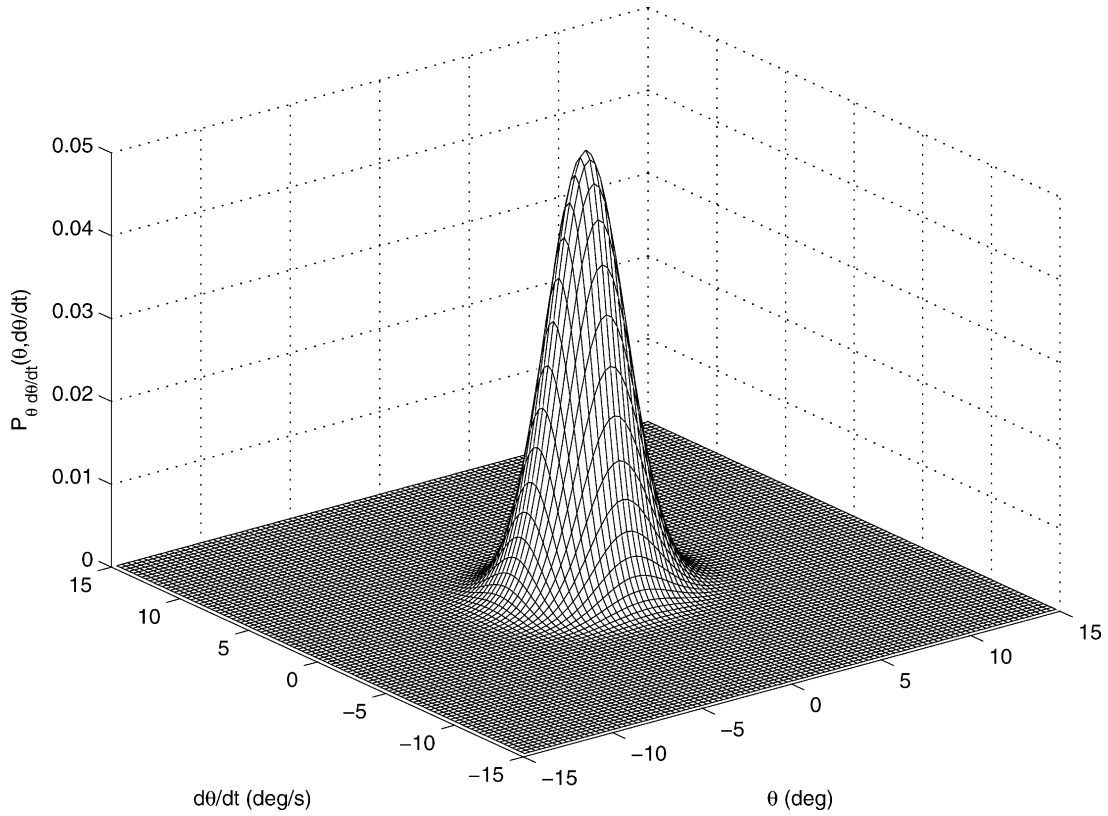


Fig. 4. Roll/roll velocity joint probability density function; significant wave height 2.74 m and mean period 15 s, $\sigma_{\theta}=1.8708^{\circ}$ and $\sigma_{\dot{\theta}}=1.6049^{\circ}/s$.

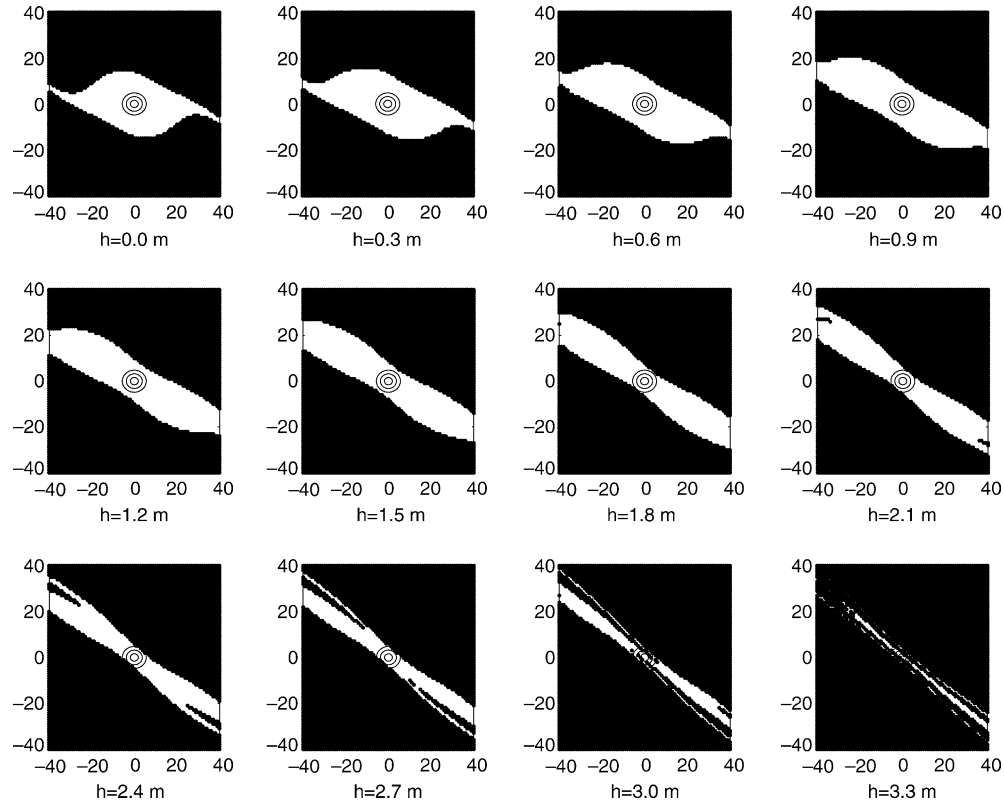


Fig. 5. Sample phase space for 12 regular sea heights and constant wave period of 15 s. One, two, and three standard deviations for initial roll and roll velocity conditions indicated with three concentric ellipses as determined for a random sea state defined by significant wave height of 2.74 m and mean period of 15 s. X and Y -axes represent roll and roll velocity, respectively.

greater magnitude where n is the number of wave cycles necessary to cause capsize. Thus one must multiply the probability of capsize for each set of initial conditions at a given wave height with the probability of attaining the n waves of equal or greater height required to cause capsize and then cumulate the probability of capsize at any given wave height. For the sample case of $h_{1/3} = 2.74$ m and $t_e = 15$ s this corresponds to overlaying the data shown in Fig. 3 on a series of phase space diagrams like Fig. 5 factoring in a third dimension corresponding to number of cycles to capsize for varying wave heights. This result is given in Fig. 6. Fig. 6 is a curve encompassing all initial conditions within three standard deviations where each individual initial condition is weighted by the probability of encountering said initial condition. Graphically, this reflects including a weighting due to Fig. 4 in addition to Figs. 3 and 5 and is represented discretely by Eqs. (10)–(12). Recall in Eqs. (10)–(12) k denotes the number of cycles to reach a given wave amplitude; therefore the time scale in Fig. 6 is found by multiplying the number of cycles by the mean period of each condition's wave excitation

$$P_{\text{cap}}\left(\sum \theta, \sum \dot{\theta}, \tilde{\zeta} = \tilde{\zeta}_{1/k}\right) = \sum_{\theta=-\pi}^{\pi} \sum_{\dot{\theta}=-\infty}^{\infty} \Delta\theta \Delta\dot{\theta} P_{\theta\dot{\theta}}(\theta, \dot{\theta}) P(\tilde{\zeta} \geq \tilde{\zeta}_{1/k})^n \tag{10}$$

$$P_{\text{safe}}\left(\sum \theta, \sum \dot{\theta}, \tilde{\zeta} \leq \tilde{\zeta}_{1/k}\right) = \prod_{\tilde{\zeta}=0}^{\tilde{\zeta}_{1/k}} \left(1 - P_{\text{cap}}\left(\sum \theta, \sum \dot{\theta}, \tilde{\zeta}\right)\right) \tag{11}$$

$$P_{\text{cap}}\left(\sum \theta, \sum \dot{\theta}, \tilde{\zeta} \leq \tilde{\zeta}_{1/k}\right) = 1 - P_{\text{safe}}\left(\sum \theta, \sum \dot{\theta}, \tilde{\zeta} \leq \tilde{\zeta}_{1/k}\right) \tag{12}$$

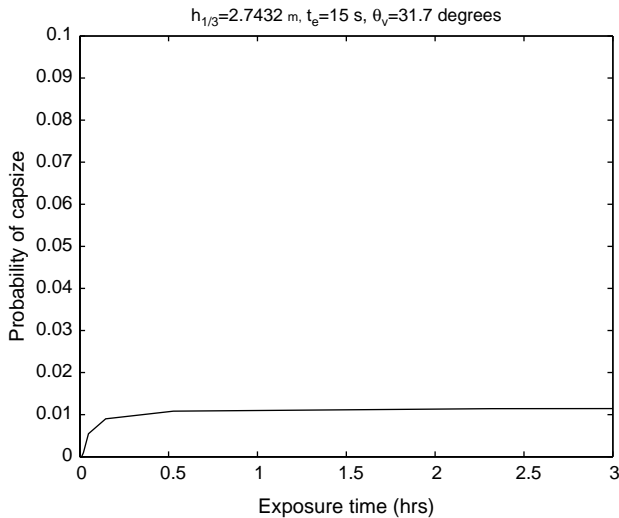


Fig. 6. Probability of capsize as a function of time for a sea state defined by significant wave height of 2.74 m and mean period of 15 s.

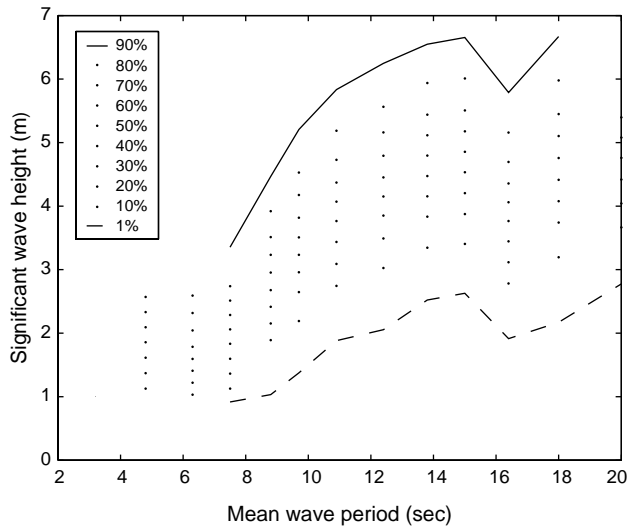


Fig. 7. Contours representing probability of capsizing over a 3 h exposure for varying sea states. Probabilities of capsizing were only calculated for documented wave height/frequency conditions (Bales et al., 1981), thus the contour lines do not extend to the limits of the plot due to the lack of observed wave heights at the lower and upper frequency limits which would result in 1 or 90% probabilities of capsizing.

Using a series of figures like that presented in Fig. 6 it is possible to calculate the probability of capsizing for the vessel over a 3 h exposure time. In this case, again one statistically weights the probability of encountering each roll/roll velocity initial condition and examines a range of significant wave height/wave frequency pairings. Fig. 7 presents contours for the studied vessel. From this we see that for the studied vessel dimensions, a conservative critical wave height of approximately 1.1 m is the safest value for all wave frequencies typically seen in the North Atlantic.

6. Conclusions

Through this form of statistical analysis one indeed notes the importance of Thompson's 'cliffs of Dover', or rapid loss of dynamic stability (Thompson, 1997). However, in this case we are presenting Thompson's critical wave height in terms of a time to encounter with probabilistic considerations for initial condition occurrences. By looking at a sample exposure time, such as 3 h, over a range of realistic wave conditions one can provide analytically and statistically viable operator guidelines as to when it is unsafe to operate due to a likelihood for a rapid loss of stability. This methodology eliminates the somewhat arbitrary nature of choice of initial condition range and thus allows one to arrive at a statistically validated choice of critical wave conditions for a given hull geometry in historically studied sea states. The use of a time-efficient simulation tool, such as the one presented, where multiple degrees of freedom are simulated under a simplified modelling approach, allows the simulation of years of potential sea states for

a vessel in a matter of days thus serving as a proof of concept for a statistical and simulation based approach to dynamic stability criteria. While some aspects of the model are admittedly simplistic, including the treatment of processes as Gaussian and the consideration of only the roll/roll-velocity parameter space, such a methodology lends insight into multi-degree of freedom capsizing analysis and serves as a proof of concept for this form of approach. If expanded upon to include a parameter sweep in all initial conditions and coupled with other probabilistic models (Atua and Ayyub, 1997; Belenky, 2000) this method would provide a basis for a realistic and accurate regulation for highly nonlinear chaotic phenomena such as vessel capsizing.

Acknowledgements

The authors wish to express their gratitude for funding on this project from the Department of Naval Architecture and Marine Engineering at the University of Michigan and the National Defense Science and Engineering Graduate Fellowship program.

References

- Atua, K., Ayyub, B., 1997. Reliability analysis of transverse stability of surface ships. *Naval Engineers Journal*, 129–141.
- Bales, S.L., Lee, W.T., Voelker, J.M., 1981. Standardized wave and wind environments for Nato operational areas. Technical report. DTNSRDC/SPD-0919-01. David W. Taylor Naval Ship Research and Development Center.
- Beck, R., Troesch, A., 1990. Students' Documentation and Users' Manual for the Computer Program SHIPMO.BM. University of Michigan, Ann Arbor.
- Belenky, V., 2000. Probabilistic approach for intact stability standards. *SNAME Transactions* 108, 123–146.
- Belenky, V., Liut, D., Weems, K., Shin, Y.-S., 2002. Nonlinear Ship Roll Simulation with Water-on-deck Proceedings: 2002 Stability Workshop.
- Chen, S.-L., Shaw, S.W., Troesch, A.W., 1999. A Systematic Approach to Modeling Nonlinear Multi-dof Ship Motions in Regular Seas, vol. 43, pp. 25–37.
- Crandall, S., Mark, W., 1963. *Random Vibration in Mechanical Systems*. Academic Press, London.
- Dillingham, J., 1981. Motion studies of a vessel with water on deck. *Marine Technology* 18 (1), 38–50.
- Falzarano, J.M., Shaw, S.W., Troesch, A.W., 1992. Application of global methods for analyzing dynamical systems to ship rolling motion and capsizing. *International Journal of Bifurcation and Chaos* 2 (1), 101–115.
- Francescutto, A., 1993. Nonlinear ship rolling in the presence of narrow band excitation, In: Falzarano, J.M., Papoulias, F. (Eds.), *Nonlinear Dynamics of Marine Vehicles*, pp. 93–102.
- Haddara, M., Wishahy, M., 2002. An investigation of roll characteristics of two full scale ships at sea. *Ocean Engineering* 29, 651–666.
- Haddara, M., Wishahy, M., Wu, X., 1994. Assessment of ship's transverse stability at sea. *Ocean Engineering* 21, 781–800.
- Hsieh, S.-R., Troesch, A.W., Shaw, S.W., 1994. A nonlinear probabilistic method for predicting vessel capsizing in random beam seas. *Proceedings of the Royal Society of London A* 446, 195–211.
- Laranjinha, M., Falzarano, J.M., Soares, C.G., 2002. Analysis of the Dynamical Behaviour of an Offshore Supply Vessel with Water on Deck, Proceedings: 21st International Conference of Offshore Mechanics and Arctic Engineering.

- Lee, Y.-W., McCue, L., Obar, M., Troesch, A., accepted for publication. Experimental and numerical investigation into the effects of initial conditions on a three degree of freedom capsizes model. *Journal of Ship Research*.
- Marsden, J.E., Ratiu, T.S., 1991. *Introduction to Mechanics and Symmetry*, second ed. Springer, Berlin.
- McCue, L., Troesch, A., 2003. The Effect of Coupled Heave/Heave Velocity or Sway/Sway Velocity Initial Conditions on Capsizes Modelling, Proceedings: Eighth International Conference on the Stability of Ships and Ocean Vehicles.
- Newland, D., 1993. *An Introduction to Random Vibrations, Spectral and Wavelet Analysis*, third ed. Longman, London.
- Obar, M.S., Lee, Y.-W., Troesch, A.W., 2001. An Experimental Investigation into the Effects Initial Conditions and Water on Deck Have on a Three Degree of Freedom Capsizes Model, Proceedings: Fifth International Workshop on the Stability and Operational Safety of Ships, September.
- Schauer, T., Romberg, B., Jiang, C., Troesch, A.W., 1995. Risk assessment of small fishing vessel trap net operations. *Marine Technology* 32 (3), 231–243.
- Soliman, M.S., Thompson, J., 1991. Transient and steady state analysis of capsizes phenomena. *Applied Ocean Research* 13, 2.
- Spyrou, K., Thompson, J., 2000. The nonlinear dynamics of ship motions: a field overview and some recent developments. *Philosophical Transactions of the Royal Society of London*, 1735–1760.
- Thompson, J., 1997. Designing against capsizes in beam seas: recent advances and new insights. *Applied Mechanics Reviews* 50, 5.
- Thompson, J., Bishop, S., Leung, L., 1987. Fractal basins and chaotic bifurcations prior to escape from a potential well. *Physics Letters A* 121.
- Wiggins, S., 1990. *Introduction to Applied Nonlinear Dynamical Systems and Chaos*. Springer, Berlin.
- Zhang, Y., Haddara, M., 1993. Parametric identification of nonlinear roll motion using roll response. *International Shipbuilding Progress* 40, 299–310.